



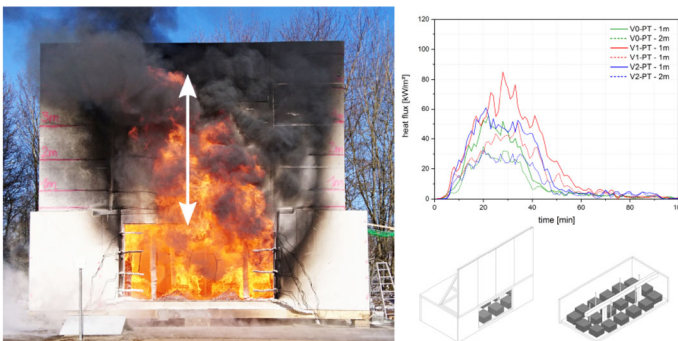
Impact of Mass Timber Compartment Fires on Façade Fire Exposure

Thomas Engel * and Norman Werther , Department of Civil and Environmental Engineering, TUM School of Engineering and Design, Timber Structures and Building Construction, Technical University of Munich, Arcisstr. 21, 80333 Munich, Germany

Received: 4 August 2022/**Accepted:** 8 November 2022/**Published online:** 13 December 2022

Abstract. This study investigates whether timber surfaces that are initially exposed to fire or partially protected timber components can lead to a more critical fire exposure on the façade. Five full-scale fire tests were carried out. Three tests with a square compartment ($4.5 \times 4.5 \text{ m}^2$) and two with a double-width compartment ($4.5 \times 9 \text{ m}^2$). The tests were conducted with a high fire load density (1085 MJ/m^2). While the first test was carried out in a non-combustible compartment, the exposed timber surfaces were subsequently increased in the other tests. The measured compartment gas temperature, heat release rate, temperature on the façade, flame heights along the façade, heat flux and velocities along the façade are presented in this publication. The influence of exposed or only initially protected timber surfaces on the fire impact on the façade is investigated with the help of these results. Finally, these findings are presented and compared with the results of other internationally conducted fire tests from literature. Additional structural fire load leads to an increase in temperatures on the façade. However, there is no significant difference in flame height between the tests. Another result was that an exposed mass timber ceiling leads to higher heat fluxes on the façade than an exposed mass timber wall.

Graphical Abstract



Keywords: Fire safety, Multi-storey timber buildings, Façades, Fire exposure, Mass timber, Exposed timber surface

*Correspondence should be addressed to: Thomas Engel, E-mail: engel@tum.de



1. Introduction

Timber constructions are increasing in popularity due to their high degree of pre-fabrication and environmental benefits. Several studies show that exposed timber surfaces or partially protected timber components can cause a fire to develop faster, be more intense, last longer and may have a relevant impact on the fire exposure on the façade than in non-combustible compartments [1, 2].

This leads to the hypothesis that more exposed timber in the form of a structural fire load can lead to more critical effects on the façade, a hypothesis that needs to be investigated further.

The fact that the most frequent mode of significant fire spread is via the façade shows just how important this aspect is [3]. This is also proven by statistics provided by German fire brigades [4, 5].

2. Analysis of Existing Previous Experimental Investigations

2.1. Reduced-Scale Fire Experiments

Gorska et al. [6, 7] investigated the effect of exposed timber walls and ceilings on the compartment fire dynamics in 24 medium-scale compartment ($0.5\text{ m} \times 0.5\text{ m} \times 0.37\text{ m}$ with opening $0.3\text{ m} \times 0.28\text{ m}$) experiments. The compartments were constructed with cross-laminated timber (CLT). The contribution of the structural timber to heat-release-rates, the temperatures on the façade, the flame-heights outside the opening and velocity fields at the opening were investigated and compared to each other within the series of experiments. A significant increase in the magnitude of the external flames and of the temperatures at the façade due to exposed timber surfaces was observed. The data indicate that exposing more CLT surfaces to fire in the compartment results in larger external flames, and consequently in higher temperatures. However, the increase in temperature is not directly proportional to the area of CLT exposed to fire. In addition, a significant increase in velocities [7] and in radiant heat fluxes were detected as more CLT panels were left exposed. “The increase of radiant heat flux, especially at lower heights closer to the opening, presents up to five-time bigger values when compared to the baseline scenario. This change implies that the façade is exposed to five times more heat, which indicates that fire spread due to ignition of the façade materials is much more likely to happen” [6].

Nothard et al. [8] investigated the influence of a combustible CLT ceiling on the compartment fire dynamics in 1/8 reduced scale fire experiments. The CLT ceiling leads to a significant increase in the rate of fire spread in the compartment. These more rapid transitions to a fully developed fire led to an earlier fire exposure at the façade [8].

Bartlett et al. [9] carried out a series of eight reduced-scale compartment fire experiments to examine the effects of the quantity and location of exposed timber on the heat fluxes to the façade from the resulting external fire plume. The compartments had internal dimensions of $700\text{ mm} \times 700\text{ mm} \times 700\text{ mm}$, and were

constructed from CLT panels and vermiculite board. It was concluded that increasing the quantity of exposed timber in the compartment results in an increased peak in the heat fluxes and increased burning durations outside. This means that there is a strong correlation between flame height and incident heat fluxes [9].

The experiments presented above show that exposed timber surfaces in the compartment lead to an increase in heat flux and flame height outside the opening. However, it should be noted that the experiments were all carried out on a reduced scale. An attempt was subsequently made to reproduce the full-scale fire tests presented in this study (Sect. 3) by experiments on a scale of 1/10. It turned out that the fire dynamics in the room, and especially on the façade, could not be reproduced appropriately [10].

2.2. Full-Scale Fire Tests

Maag et al. [11] carried out a series of fire tests on wooden modular hotels with light timber frame walls and ceilings to investigate the behavior of modular hotels subjected to natural fires. The light timber frame walls and ceilings had non-combustible and combustible linings. The influence of combustible linings on to the fire severity was clearly observed after flashover occurred. The external flame was more intense for the module with combustible wall and ceiling linings than for the modules with non-combustible wall and ceiling linings. Consequently, the total energy release was significantly lower in the tests with non-combustible linings and the fire spread to the upper module after about 40 min. In the test with combustible linings, on the other hand, the fire spread after just eight minutes. When evaluating the results, it must be taken into account that window panes were installed and the fire propagation to the upper floor depended on the bursting of the panes [11, 12].

Su and Lougheed [13] conducted four full-scale fire tests with two compartments made of light timber frames, one made of lightweight steel-frames and one made of CLT. As part of these tests, they measured the heat flux on the façade 3.5 m above the compartment openings. The measurements concluded that the involvement of the timber joists and OSB linings in the fire led to the increase of the heat release rate (HRR) and heat fluxes to the façade and adjacent structures [13].

Hakkarainen [14] investigated the gas temperature development and charring behavior of timber frame and mass timber compartments. For this purpose, she conducted three full-scale fire tests with glued laminated timber (GLT) wall and ceiling elements and one test with light timber frame elements. In the first test (Test 1), all GLT walls and the ceiling were unprotected and directly exposed to the fire. In the other tests, the walls and ceilings were protected by gypsum-plasterboards of different thicknesses (thickness increasing from Test 2 to Test 4).

In Test 1 and 2, the heat flux showed an increasing trend until the fire was extinguished. Test 3 and 4 exhibited heat flux maxima approximately 20 min to 30 min after flashover, followed by a decrease of the heat flux when the movable fire load was consumed, as shown in Fig. 1.

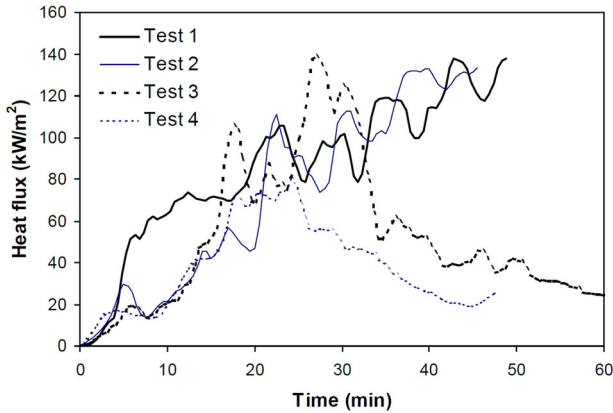


Figure 1. Heat flux measurements on the façade 2.2 m above the opening from the four tests [2] based on [13].

Based on Hakkarainen's visual observations and the energy balance considerations, she concluded that a large part of the pyrolysis gases burned outside the compartment in the case of exposed or partially protected (test 1 and 2) timber surfaces. According to the calculation, about 15% of the combustion took place outside the room in the case of the protected timber structure, while the proportion of external combustion in the unprotected structure was about 50% [14].

Su et al. [15] investigated, among other things, the influence of the exposed timber surface in five large-scale fire tests. The impact on the façade was not part of the investigation. However, they came to the conclusion that flashover and fire impingement on the facade occurs earlier in the case of exposed CLT [15]. This assumption is confirmed in Hadden et al. [16]. He further concludes that the addition of pyrolysis gases from the exposed timber surfaces will prolong the compartment fire and potentially increase the HRR rate both inside and outside the compartment [16].

Su et al. [17] conducted six large CLT compartment fire tests to quantify the CLT contribution to compartment fires. In all the tests with unprotected und directly exposed CLT surfaces, flashover occurred earlier, the fully developed fire lasted longer and the HRRs and heat fluxes to the exterior façade were higher than in the baseline tests with protected CLT surfaces [17].

The influence of combustible surfaces and ventilation factors on the dynamics of compartment fires (including external flaming) was investigated as part of the Épernon Fire Tests [18]. The test series includes three standard furnace fire resistance tests and six compartment fire tests with loadbearing reinforced concrete slabs and loadbearing CLT slabs. The six compartment tests can be divided into three groups, Scenario 1, Scenario 2 and Scenario 3. Each of these groups includes two tests under the same conditions, investigating the influence of a CLT slab compared to a concrete slab as a ceiling. Scenarios 1–3 differ in the respective ventilation conditions [18].

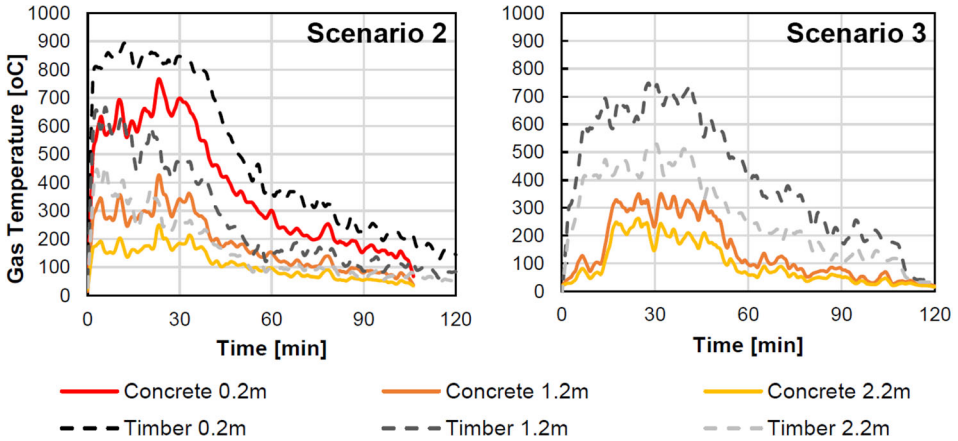


Figure 2. Temperatures at the centerline of the mock-up façade for Scenarios 2 (left) and 3 (right) [18].

A mock-up façade was installed above the compartment opening in order to monitor external flaming for the four compartment tests of Scenarios 2 and 3 [18, 20–23]. The incident heat flux to the façade was approximately three times greater when a timber ceiling was used instead of a concrete ceiling. According to the report, this is due to the additional pyrolysis by the burning CLT slabs, which burns in the outer plume due to a lack of oxygen in the compartment [18, 19].

The gas phase temperatures above the openings are shown in Fig. 2. As with the heat fluxes, the presence of an exposed timber ceiling significantly increases the temperatures in the external fire plume. It can be seen that the temperatures fall as a function of the height [18, 19].

Brandon et al. [24] and Sjöström et al. [25] conducted five full-scale compartment fire tests within CLT and GLT constructions. Four of the tested compartments represent a typical residential compartment. The other tested compartment aimed to be representative of office occupancy. The residential fires tests had unprotected, directly exposed mass timber areas of 54 m² for test 1, 91 m² for test 2, 96 m² for test 3 and 97 m² for test 5. Test 4 represented an office occupancy with large ventilation openings and an exposed mass timber area of 97 m². Along with other components in all tests, the timber ceiling was completely exposed to fire from the beginning of the tests. Among many other measurements, exposure to the façade above the openings was investigated and the results were presented in a separate report by Sjöström et al. [25]. An increase of roughly 40 m² of exposed surface area (from (from 54 m² to 94 m²) resulted in a temperature increase of 100 °C to 130 °C at the façade at all heights up to 3.5 m above the opening in these tests. Additionally, an increased fire plume height of up to 1 m was observed, as shown in Fig. 3. The most significant effect of increasing the exposed areas of the timber surface in the compartment was a prolonged duration of the fully developed fire phase [24, 25].

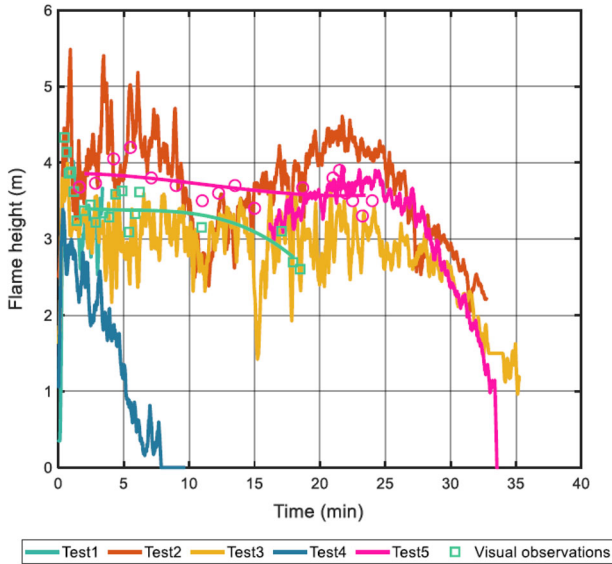


Figure 3. Flame heights determined by data obtained by image analysis or visual observations [25].

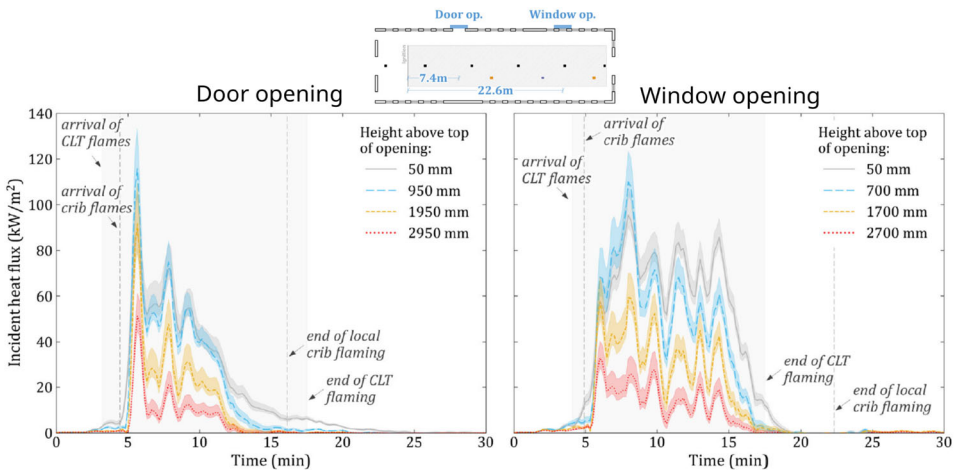


Figure 4. Incident heat fluxes to the façade measured at various heights above the opening soffit (CodeRed #01) [26].

Kotsovinos et al. [26] investigated the fire dynamics of large compartments. The test CodeRed #01 was carried out inside a large open-plan compartment with a floor area of 352 m². The compartment had a fully exposed CLT ceiling and GLT columns. Previously, the research team had already carried out two comparable tests in non-combustible compartments [27, 28]. In a first comparison, the research

team concluded that the CLT ceiling impacts the total HRR substantially, nearly doubling the peak HRR from 69 MW [27] and 58 MW [28] to 121 MW [26]. This extra HRR impacts the amount of external flaming. External flames were observed 6 min after ignition of roughly 2.5 to 3 m in height. An initial visual comparison showed an increase in flame lengths due to the presence of exposed timber surfaces. Figure 4 shows the heat flux on the façade for the door and window opening [26].

Kotsovinos et al. [29] investigated the influence of the ventilation in another compartment fire test, which was similar in geometry and fire load to the previously cited CodeRed #01 [26]. For this CodeRed #02 test, the opening factor was reduced from $0.071 \text{ m}^{1/2}$ to $0.039 \text{ m}^{1/2}$. The differences in ventilation resulted in higher external flames (3 m to 3.5 m) and the flames protruded much further (laterally) from the compartment. In addition, the duration of the external flames was longer. A direct comparison of the heat flux on the façade of CodeRed #01 and CodeRed #02 is given by comparing Figs. 4 and 5.

3. TIMpuls Full-Scale Compartment Fire Tests

3.1. Aim of the Study

The TIMpuls full-scale compartment fire tests serve as evidence of the knowledge and findings gained during the three-year research project [30]. The load-bearing capacity, compartmentation, self-extinguishing properties and extinguishing by the fire brigade (post-fire behavior) as well as the limitation of the spread of fire were investigated. Compared to the full-scale compartment fire tests described above, the high fire load density of 1085 MJ/m^2 required for residential occupancy can be considered as a special feature of the TIMpuls fire tests. The variation between exposed, initially protected and fully encapsulated timber elements and their influence on the fire dynamics is of particular importance within the test campaign.

The aims of the TIMpuls full-scale compartment fire tests are:

- Verification of the results of previously conducted furnace tests in a real fire compartment
- Influence of exposed or only initially protected timber surfaces on the fire dynamics
- Behavior of the fire protection lining and its protection times under natural fire conditions
- Self-extinguishing and post-fire behavior of timber constructions
- Extinguishability of typical timber constructions by the fire brigade
- Investigation of the fire impact on the façade and on the stories above the compartment fire due to the additional structural fire load
- Investigation of the effects of structural fire protection measures in element joints and joints to other building components
- Evaluation of the compartmentation (fire and smoke) under natural fire exposure

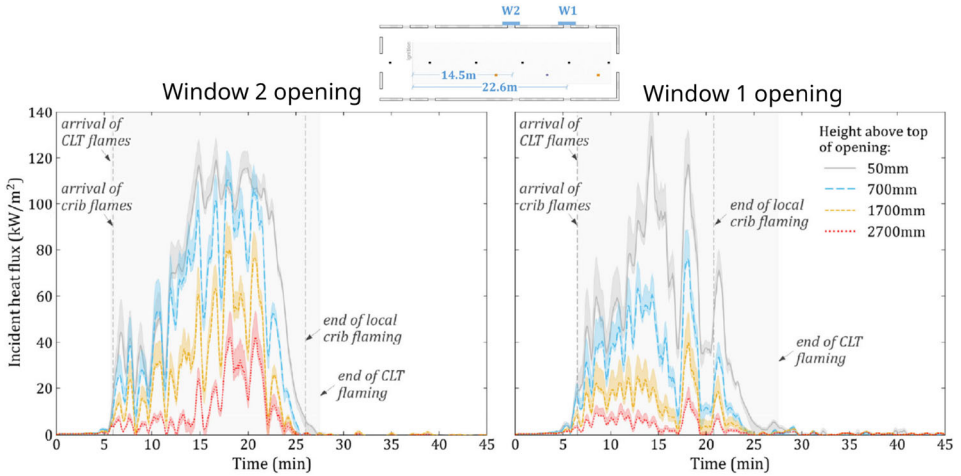


Figure 5. Incident heat fluxes to the façade measured at various heights above the opening soffit (CodeRed #02) [29].

This paper presents the investigation into the influence of additional structural fire loads on the façade and the stories above the fire compartment of origin.

3.2. Test Set-Up

3.2.1. General The first test serves as a reference test and is intended to represent a non-combustible building, e.g. made of masonry or reinforced concrete. All structural elements were encapsulated by 2×25 mm Gypsum plasterboard type F. In the other four tests, different combinations of timber constructions, such as CLT, glued-laminated timber (GLT) and light timber frame (LTF) were used, each in combination with gypsum plasterboard type F (GPF) or gypsum fiberboard (GF) or exposed, as shown in Table 1. A detailed overview of the wall and ceiling structures used in the tests is given in Table 4 of Appendix.

3.2.2. Compartment The internal dimension of the floor area was 4.5×4.5 m² (LxW) for the first three compartment fire tests V0, V1, V2 and 4.5×9 m² (LxW) for two following compartment fire tests V3, V4. The geometric ratio of the floor area of one to two made it possible to observe the spatial influence on the fire dynamics, as shown in Figs. 6, 7, 8, 9, 10 and 11. In order to represent typical room heights, the internal dimension of the test rooms is approx. 2.4 m, as shown in Table 1.

All compartments have just one window opening. The opening is 2.4×2.2 m² (W \times H) in the small room (4.5×4.5 m²) and 4.2×2.2 m² (W \times H) in the large room (4.5×9 m²). This results in a constant opening factor of 0.094 m^{1/2}. The opening was open from the beginning of each test.

The floor covering was made of gypsum plasterboard or gypsum fibreboard.

Table 1
Description of the Individual Experimental Set-Ups

Test	V0	V1	V2	V3	V4
Compartment size (W × L × H)	4.5 m × 4.5 m × 2.4 m			4.5 m × 9.0 m × 2.4 m	
Floor space	20.25 m ²			40.5 m ²	
Opening size (W × H)	2.4 m × 2.2 m			4.2 m × 2.2 m	
Fire load density	1085 MJ/m ²				
Wall 1	100 mm CLT 2 × 25 mm GPF	100 mm CLT 18 mm GF	150 mm CLT	140 mm LTF 2 × 12.5 mm GF + 12 mm OSB	150 mm CLT
Wall 2	100 mm CLT 2 × 25 mm GPF	100 mm CLT 18 mm GF	140 mm LTF 2 × 18 mm GF	140 mm LTF 2 × 18 mm GF + 12 mm OSB (half wall)	140 mm LTF 2 × 18 mm GF
Wall 3	100 mm CLT 2 × 25 mm GPF	100 mm CLT 18 mm GF	150 mm CLT	140 mm LTF 2 × 18 mm GPF	140 mm LTF 2 × 18 mm GPF
Wall 4	100 mm CLT 2 × 25 mm GPF	100 mm CLT 18 mm GF	140 mm LTF 2 × 18 mm GF	140 mm LTF 2 × 18 mm GF	140 mm LTF 2 × 18 mm GF
Ceiling	180 mm GLT 2 × 25 mm GPF	180 mm GLT	220 mm LTF 2 × 18 mm GF	180 mm GLT	180 mm GLT
Linear components	–	–	–	–	2 × Column ^a 1 × Beam ^b
Exposed surface (initial) ^c	–	35%	37%	42%	58%

CLT cross-laminated timber, *LTF* light timber frame, *GLT* glued-laminated timber, *GPF* gypsum plasterboard type F, *GF* gypsum fiberboard, *OSB* oriented strand board

^aColumn—300 × 300 mm² GLT

^bBeam—300 × 320 mm² GLT

^cAs percentage of the total compartment surfaces excluding floor and window opening

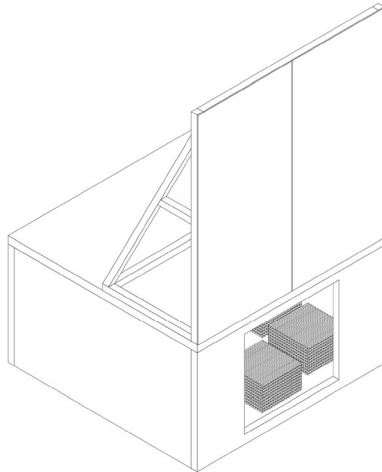


Figure 6. Perspective V0, V1, V2.

3.2.3. *Fire Load* For the tests, a fire load density was selected that is appropriate for residential buildings. According to [31], this results in a characteristic fire load density of 1085 MJ/m² for the 90% quantile.

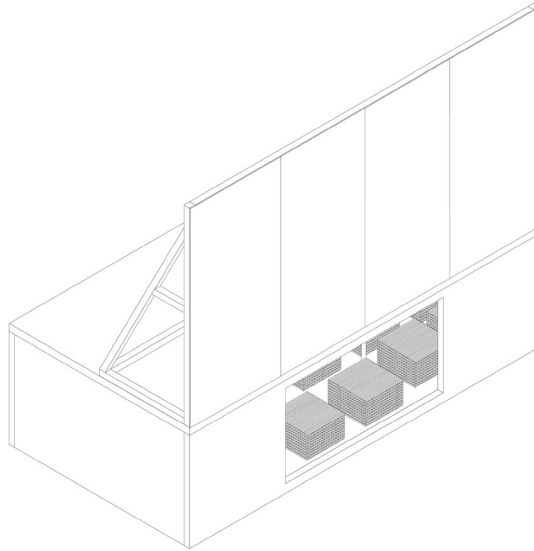


Figure 7. Perspective V3 and V4.

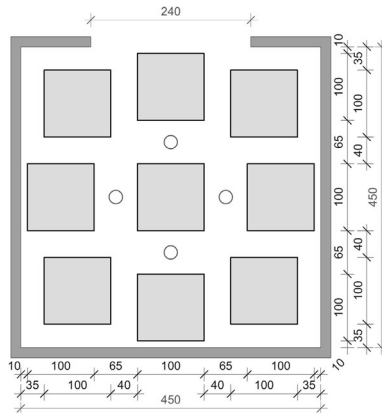


Figure 8. Floor plan with arrangement of the 9 wooden cribs and the four thermocouple trees (circle) for tests V0, V1, V2 (in cm).

The fire load was designed in the form of wooden cribs. The floor area of the individual wooden cribs that are evenly distributed in the compartment is $1 \times 1 \text{ m}^2$ each. They are made of sticks of the dimensions $W \times H = 40 \times 40 \text{ mm}^2$. The surface to air ratio of the cribs is 1:1. Taking into account the wood moisture and the density of the wood, the fire load of 1085 MJ/m^2 described above corresponds to approx. 74 kg/m^2 of wood. In total, approx. 1.5 tons of wood were used in the small compartment ($4.5 \times 4.5 \text{ m}^2$) and approx. 3 tons of wood in the large compartment ($4.5 \times 9 \text{ m}^2$). The arrangement of the wooden

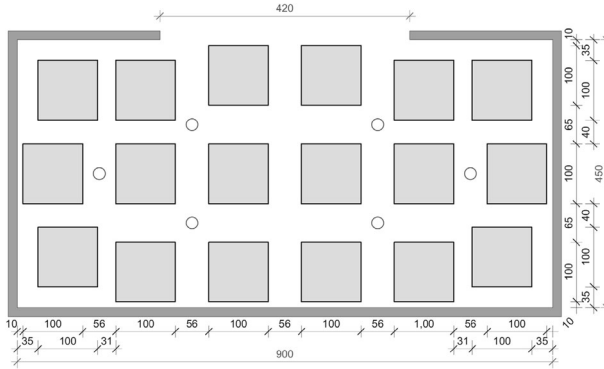


Figure 9. Floor plan with arrangement of the 18 wooden cribs and the six thermocouple trees (circle) for test V3 (in cm).

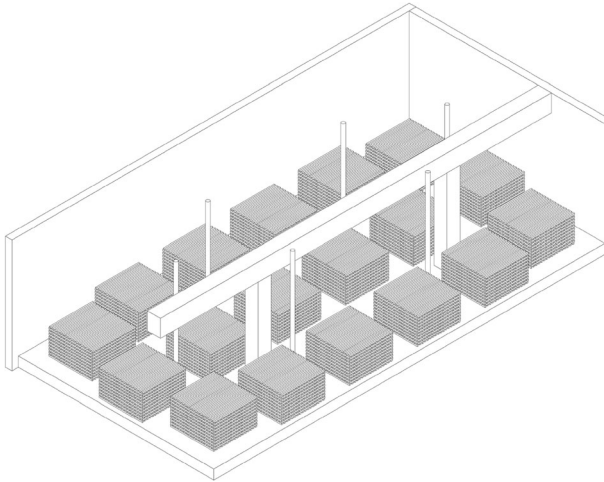


Figure 10. 3D-model of test V4.

cribs in the compartments are shown in Figs. 8, 9 and 11. Due to the very high fire load, the tests that were carried out can be defined as unique. This is also evident when comparing the fire load densities for Europe specified in Eurocode 1 or in the respective national annexes, as shown in Table 5 of Appendix.

3.2.4. Façade Shield The façade shield above the window opening was constructed from cement-bonded sandwich panels mounted on a timber substructure. The use of cement-bonded sandwich panels was intended to reduce the influence of evaporating water steam to the measurements.

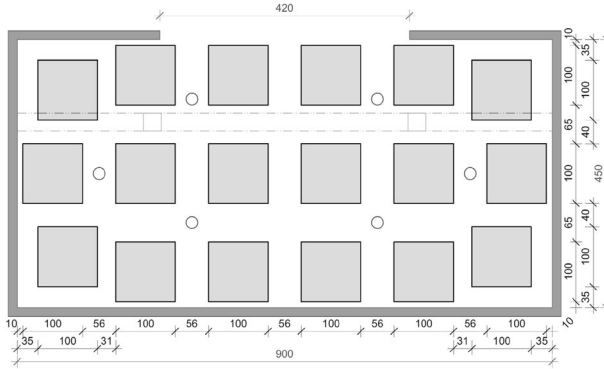


Figure 11. Floor plan with arrangement of the 18 wooden cribs and the six thermocouple trees (circle) for test V4 (in cm).

3.3. Test Procedure

Two wooden cribs arranged along wall 3, starting from the corner of wall 2 and 3, were always used for ignition. The two wooden cribs were equipped with two ignition trays $39 \times 39 \times 1200 \text{ mm}^3$ ($W \times H \times L$) with 200 ml of isopropanol in each. The four trays are ignited directly one after the other and then the test time started. All observations were documented during the test time.

The tests V1, V2, V3 and V4 did not self-extinguish. They were therefore all extinguished by the fire brigade.

The weather data for the individual tests are provided in Table 6 of Appendix.

3.4. Instrumentation

Extensive instrumentation was arranged to measure the influence of the fire dynamics and the thermal exposure on the structure. The temperature development of the gas in the compartment, on the façade and within the building components as well as element joints and joints to other building components was measured, as was the incident heat flux received by the ceiling, by wall 1 and by the façade. The gas flow velocities were also measured in the opening, within the compartment and on the façade as was the separate mass losses for the floor and other components. A total of up to 300 type-K thermocouples, 6 plate thermometers, 10 bidirectional probes and 6 cameras were used as part of each fire test.

Following a more detailed description of the instrumentation used in the tests, the effect of the fire on the façade is described.

Four thermocouple trees each were arranged in the compartment test for V0, V1, V2 and six for V3 and V4, as shown in Figs. 8, 9 and 11. To measure the gas temperature, five thermocouples were arranged per thermocouple tree at heights of 50, 100, 150, 200 and 230 cm. Sheathed thermocouples of type K according to EN 60584-1 [32] with an outer diameter of 1 mm were arranged for V0 and V1, and with an outer diameter of 3 mm for V2, V3, V4. A plate thermocouple was

installed 10 cm below the ceiling in all tests. This corresponds to a height of 230 cm in relation to the compartment.

In order to determine the mass loss, the floor and the structural components (walls, ceiling) were each placed on decoupled floor frames and these frames were supported on individual load cells. A total of eight load cells were positioned under the frames for V0–V2 and 10 for V3 and V4.

30 thermocouples, two plate thermocouple and two bidirectional probes for measuring the gas flow velocity were placed on the façade shield for V0–V2 and 54 thermocouples, two plate thermocouple and two bidirectional probes for V3 and V4. Sheathed thermocouples of type K according to EN 60584-1 [32] with an outer diameter of 3 mm, plate thermocouple according to EN 1363-1 [33] and bidirectional probes of the type BS11 according to [34] were used.

The thermocouples were positioned at a distance of 20 mm from the surface of the façade, the plate thermocouple and the bidirectional probes at a distance of

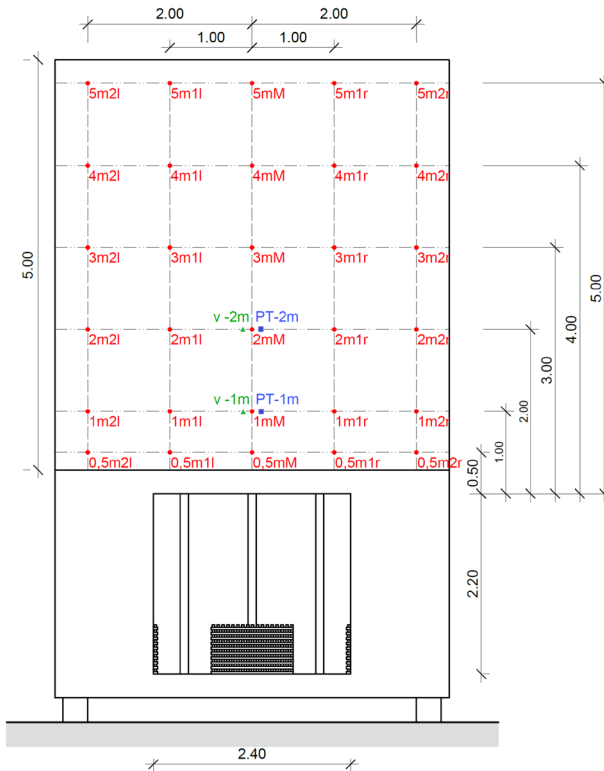


Figure 12. Façade shield V0-V2 with dimensions and measuring points; unit of dimensions m] (red ● = sheathed thermocouples, blue ■ = plate thermocouple, green ▲ bidirectional probes) (Color figure online).

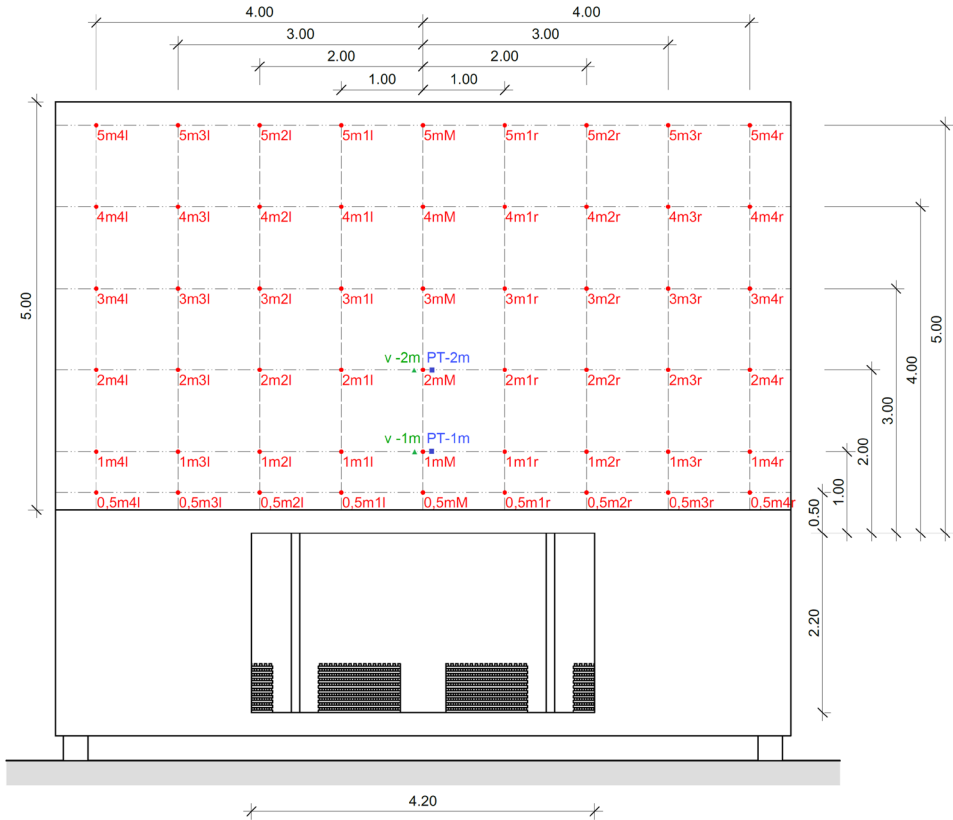


Figure 13. Façade shield V3 and V4 with dimensions and measuring points; unit of dimensions [m] (red ● = sheathed thermocouples, blue ■ = plate thermocouple, green ▲ = bidirectional probes) (Color figure online).

50 mm. They were fixed to a taut wire in front the façade. Figures 12 and 13 show the positions of the thermocouples.

4. Results of the Fire Tests

4.1. Gas Temperature

Figures 14, 15, 16, 17 and 18 show the gas temperatures in the compartment at different heights for each test. The measurements of the thermocouple (TC) trees are presented as an average value over the four trees (V0–V2) or the six trees (V3 and V4). In addition, the plate thermocouple (PT) on the ceiling is also shown.

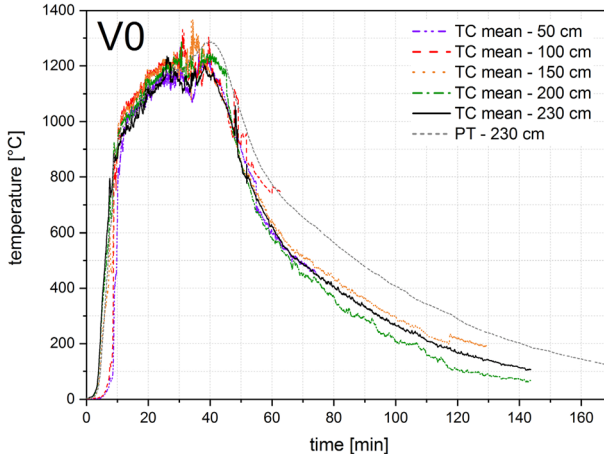


Figure 14. Gas temperatures for V0 in the compartment at different heights.

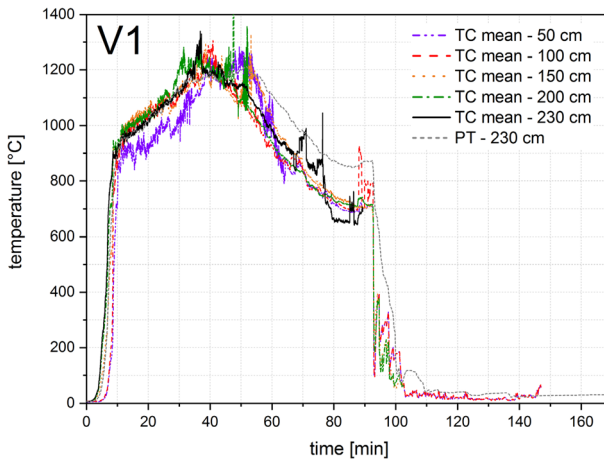


Figure 15. Gas temperatures for V1 in the compartment at different heights.

4.2. Heat Release Rate

The HRR from the measurement data of the mass loss is calculated by determining the mass loss rate and assuming a calorific value of 17.28 MJ/kg, a wood moisture content of 14% and a combustion efficiency of 0.9. Due to the strongly fluctuating measurement data, a moving average was first formed over 9 measurement cycles (recording frequency 1 s). The measurement data were then used as 25 min average values to calculate the HRR, as shown in Figs. 19 and 20 [35].

An existing strong oscillation can be seen despite the smoothing measures for the calculated HRRs of the floor (movable fire loads) in Fig. 19 and the structural

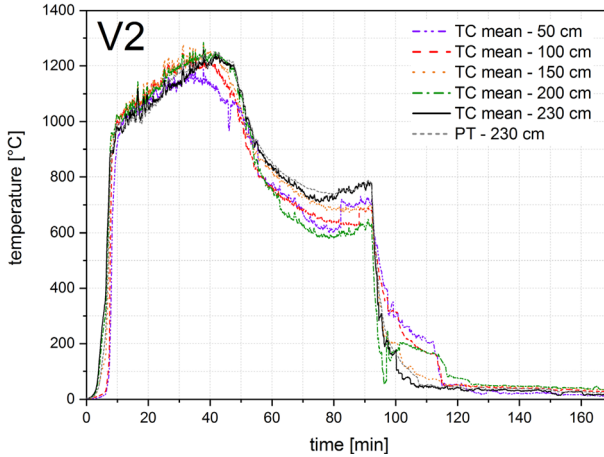


Figure 16. Gas temperatures for V2 in the compartment at different heights.

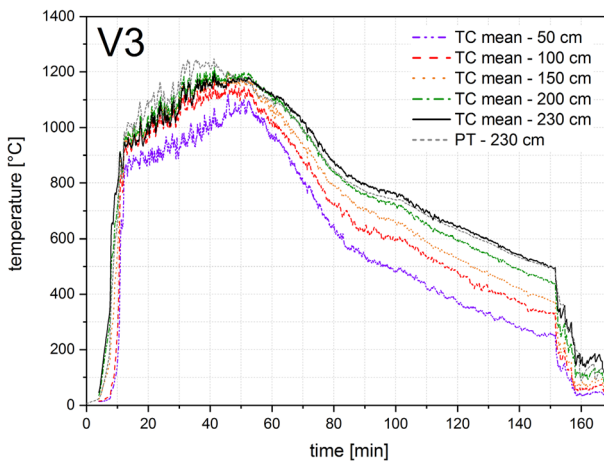


Figure 17. Gas temperatures for V3 in the compartment at different heights.

components (structural fire load) in Fig. 20. Furthermore, it must be taken into account that the recorded data of the mass loss includes the dehydration loss as well as the falling off of lining parts. The HRRs shown, especially for the structural fire load, are therefore burdened with an unnamable imprecision.

In order to describe the influence of the structural fire load more precisely, the HRR from the combustible structure was determined mathematically based on the charring rate. The following assumptions were made for the determination: (I) charring starts at 300°C [36], (II) the protection time of a lining corresponds to the time until 300°C is reached behind the lining (t_{ch} [36]), (III) the failure time of

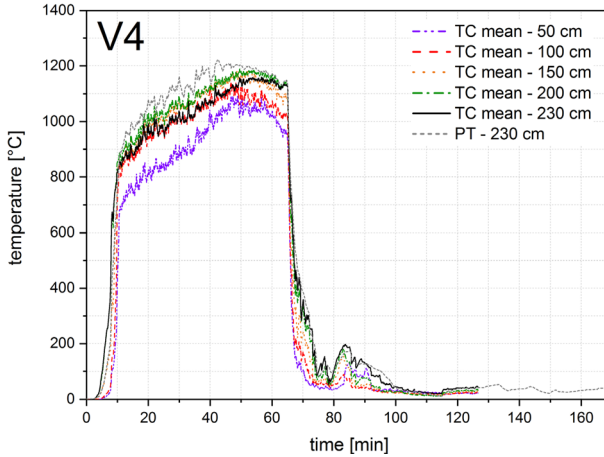


Figure 18. Gas temperatures for V4 in the compartment at different heights.

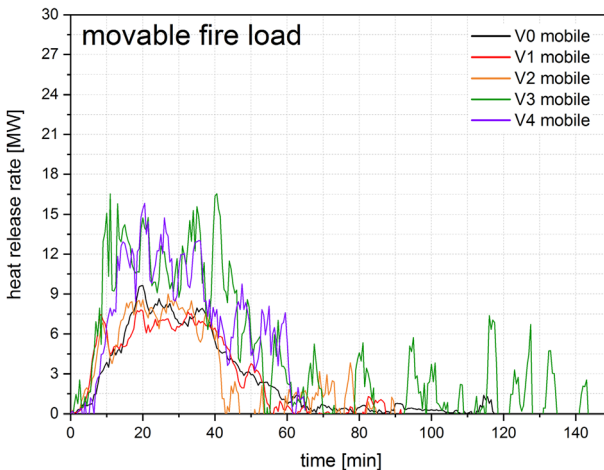


Figure 19. Comparison of heat release rates V0-V4 for the floor (movable fire load).

the fire protection lining corresponds to the time until the difference between gas temperature in the compartment and measured temperature behind the lining is less than 50°C [37] (t_f [36]) and IV) a reduced charring rate of 70% is assumed between t_{ch} and t_f (k_2 [36]). The residual cross-section of the timber components was recorded measured after the tests and the surface area of the timber components is known, as shown in Table 1 and in Tables 4 and 7 of Appendix. Mean values were determined.

The HRR is calculated with the help of this information and the aforementioned specifications for calorific value, wood moisture and combustion efficiency,

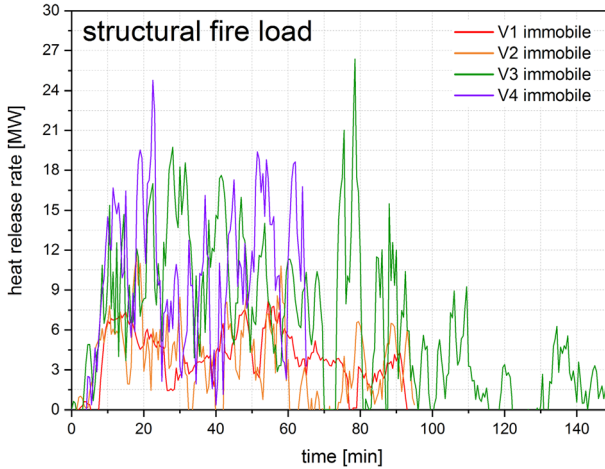


Figure 20. Comparison of heat release rates V0-V4 for the structural components (structural fire load).

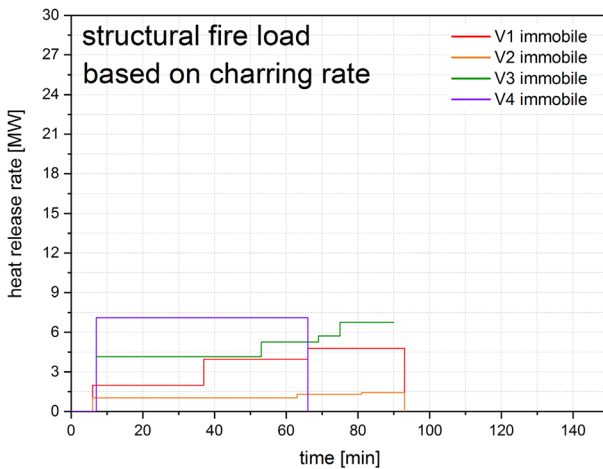


Figure 21. Comparison of heat release rates V0-V4 for the structural fire load derived from measured char depth at the end of the test.

in connection with an assumed density of wood of 450 kg/m^3 , as shown in Fig. 21. It should be noted that the calculation is based on the same assumptions for solid timber, light timber frame components and OSBs. Charring is assumed to be constant over time. In the case of V3, calculations are only made up to the 90th minute, as there is no constant charring at this point because there is no longer a movable fire load. These assumptions also lead to uncertain results. However, they should provide a trend and enable comparability. For a better comparison of the two approaches to determining the HRR (mass loss vs. char-

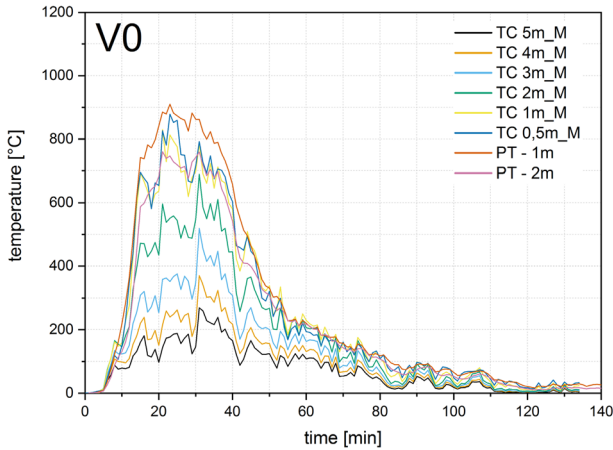


Figure 22. Temperature-time diagram of V0 façade for measuring points located centrally above the opening at different heights.

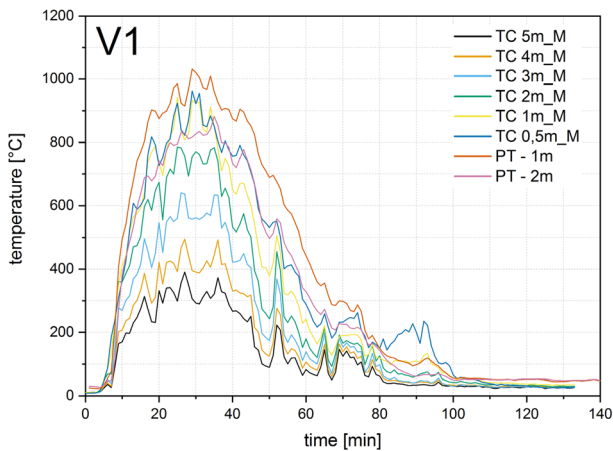


Figure 23. Temperature-time diagram of V1 façade for measuring points located centrally above the opening at different heights.

ring rate), the results are compared directly to each other in Figs. 4, 41, 42 and 43 of Appendix. It can be stated that the results have a similar range of values.

4.3. Façade Temperatures

Figures 22, 23, 24, 25 and 26 show the temperature curves at different heights along the façade. For a better overview, the measured values are presented as averages over one minute (recording frequency 10 s) and only the measuring points located centrally above the opening (thermocouples (TC) at heights of 0.5, 1, 2, 3, 4 and 5 m above the lintel) and the two plate thermocouples (PT) are

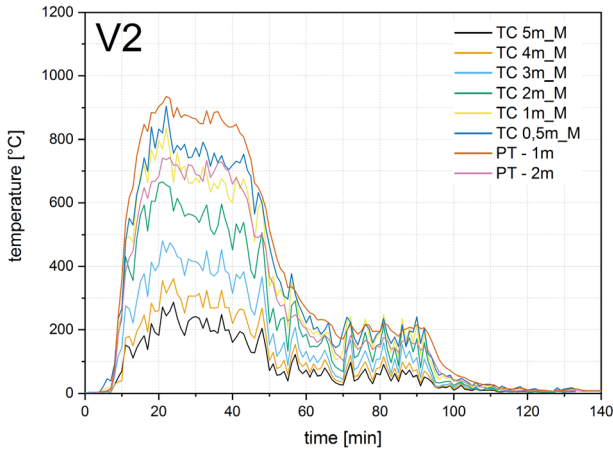


Figure 24. Temperature-time diagram of V2 façade for measuring points located centrally above the opening at different heights.

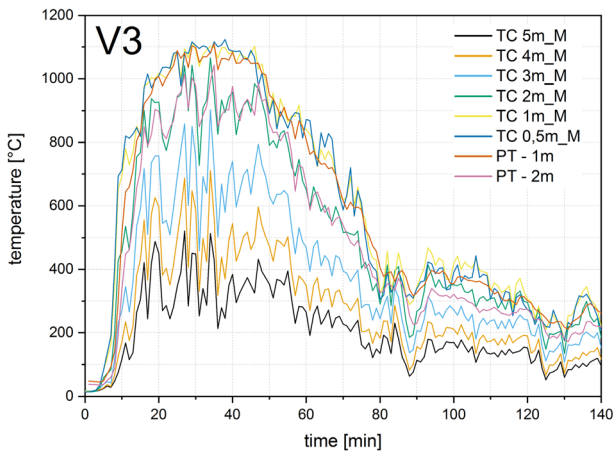


Figure 25. Temperature-time diagram of V3 façade for measuring points located centrally above the opening at different heights.

shown. The development of the external gas temperature of the tests during the first 60 min for the measuring points which were located centrally above the opening at different heights are shown in Figs. 27 and 28.

4.4. Flame Heights

The flame heights above the opening were measured visually. For this purpose, height marks were placed on the façade shield and the flame heights were observed at 30-s intervals as a weighted average [38]. A weighted moving average

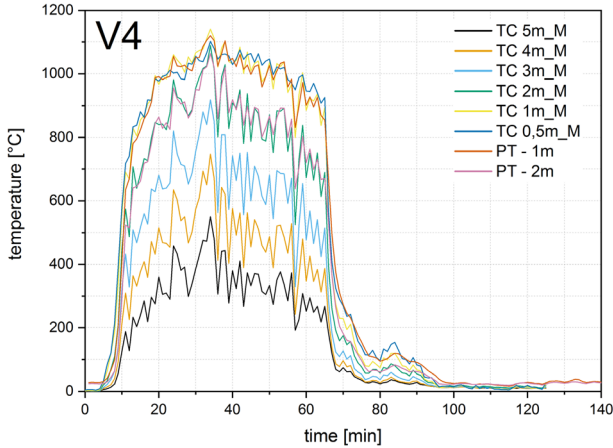


Figure 26. Temperature-time diagram of V4 façade for measuring points located centrally above the opening at different heights.

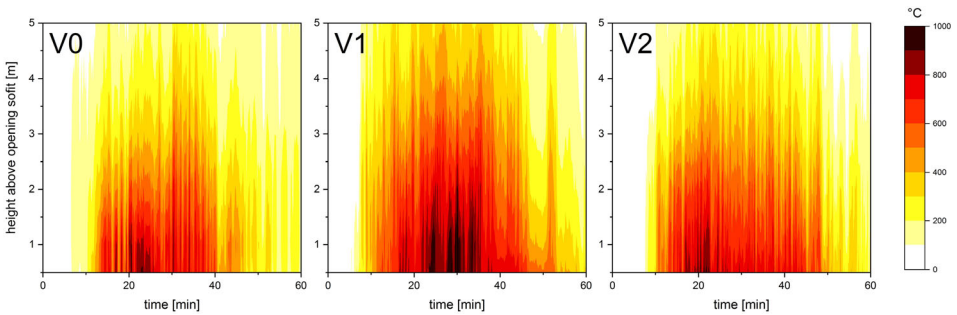


Figure 27. External gas temperature development throughout the first 60 min of V0, V1 and V2 for the measuring points located centrally above the opening at different heights.

from two data points was chosen for better visualization, as shown in Figs. 29 and 30. The flame heights can be seen in the videos of the digital appendix.

4.5. Heat Flux on the Façade

The incident heat fluxes were calculated by converting the temperatures measured by the two plate thermocouples (PT), placed on the façade centrally 1 and 2 m above the opening, as shown in Figs. 12, 13 and Sect. 4.3, according to the method used by Häggkvist et al. [39] and Ingason et al. [40] using Eq. (1):

$$\dot{q}_{inc}'' = \sigma T_{PT}^4 + \frac{(h + K_{PT})(T_{PT} - T_{\infty}) + C_{PT} \frac{dT_{PT}}{dt}}{\varepsilon_{PT}} \quad (1)$$

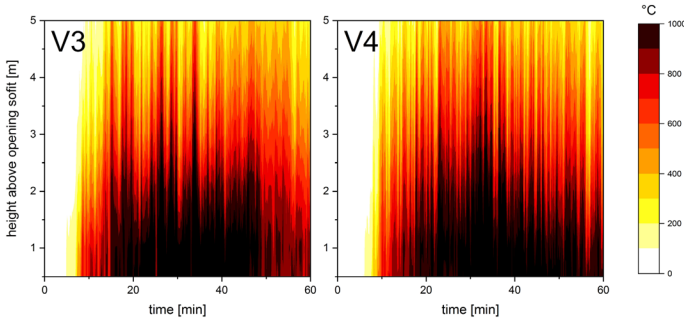


Figure 28. External gas temperature development throughout the first 60 min of V3 and V4 for the measuring points located centrally above the opening at different heights.

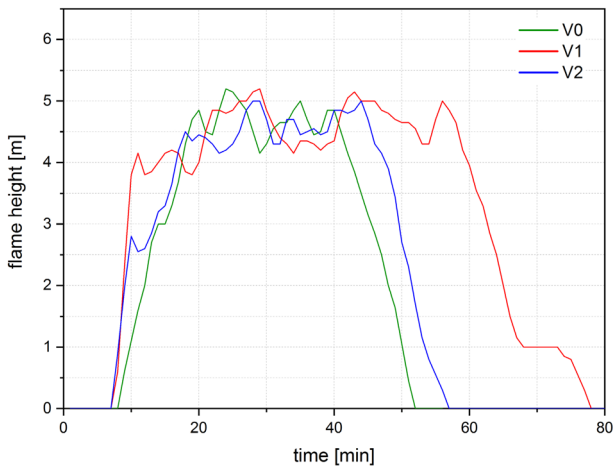


Figure 29. Flame heights above the opening for V0, V1 and V2.

where σ is the Stefan–Boltzmann constant ($5.67 \times 10^{-8} \text{ J/m}^2 \text{ K}^4$), T_{PT} is the temperature of the PT, h is the convective heat transfer coefficient ($10 \text{ W/m}^2 \text{ K}$), K_{PT} is the effective heat transfer coefficient due to conduction ($8 \text{ W/m}^2 \text{ K}$), T_{∞} is the ambient temperature, C_{PT} is the heat capacity of the PT ($4200 \text{ J/m}^2 \text{ K}$) and ε_{PT} is the emissivity of the PT surface (0.8). Note: When comparing directly with results from other research, the uncertainties or inaccuracies regarding emissivity = (0.7 to 0.9) and heat transfer coefficient = ($5 \text{ J/m}^2 \text{ K}$ to $25 \text{ J/m}^2 \text{ K}$) must be taken into account [26].

The heat flux is shown as an average over one minute (measuring frequency 25 s) for better visualization, as shown in Figs. 31 and 32.

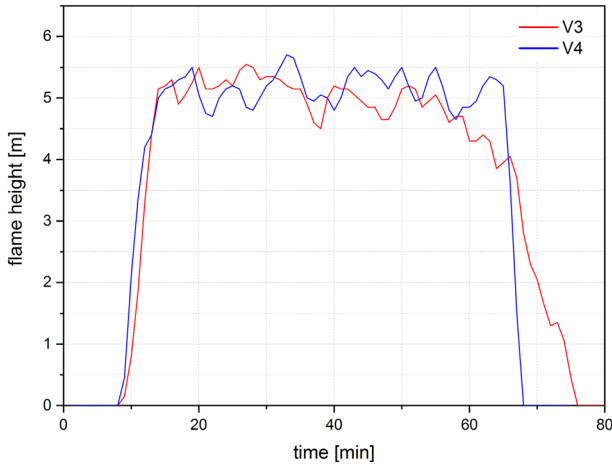


Figure 30. Flame heights above the opening for V3 and V4.

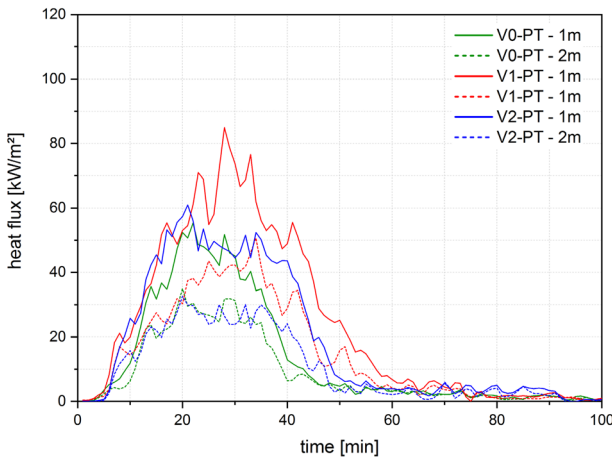


Figure 31. Heat flux measured centrally above the opening at a height of 1 and 2 m for V0, V1 and V2.

4.6. Gas Flow Velocities

The gas flow velocities on the façade were measured using bidirectional probes placed centrally above the opening at a height of 1 and 2 m, as shown in Figs. 33 and 34. The probes measure the differential pressure caused by a flow movement at the probe and calculate a direction-dependent flow velocity accordingly using Eq. (2) [30, 34]:

$$V = \sqrt{\frac{2\Delta p T}{p_0 T_0}} \quad (2)$$

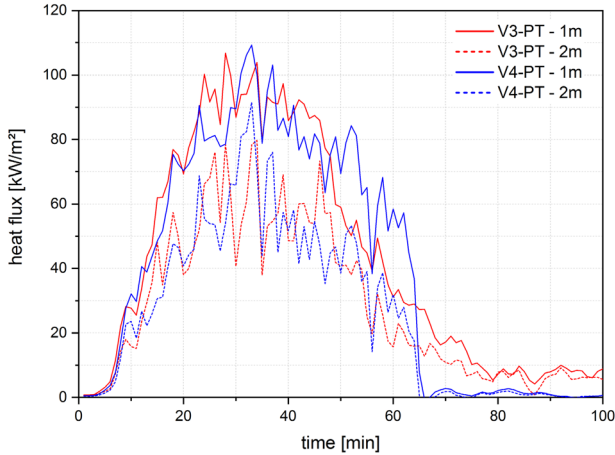


Figure 32. Heat flux measured centrally above the opening at a height of 1 and 2 m for V3 and V4.

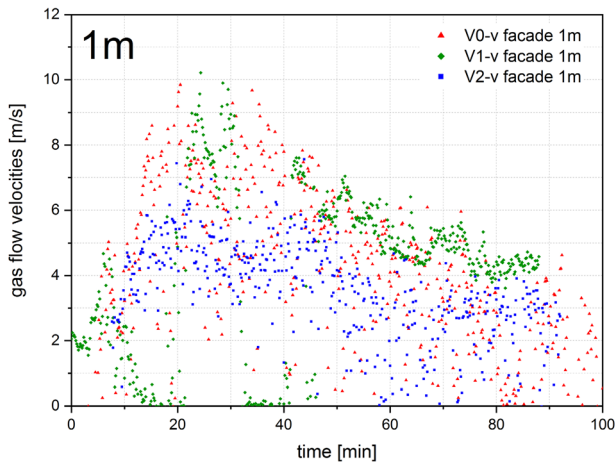


Figure 33. Comparison of the gas flow velocities on the façade at 1 m height of V0, V1 and V2.

Equation (2) is derived from the Bernoulli equation, where p_0 is the standard density of air (1.293 kg/m³), T_0 is the temperature at 0°C (273.15 K), T is the measured temperature and Δp is the differential pressure.

It should generally be noted that the bidirectional probes are sensitive to weather conditions. The evaluation of the measurement data in test V3 and V4 showed that some of the probes failed or delivered incorrect results. For this reason, these results V3 and V4 are not shown.

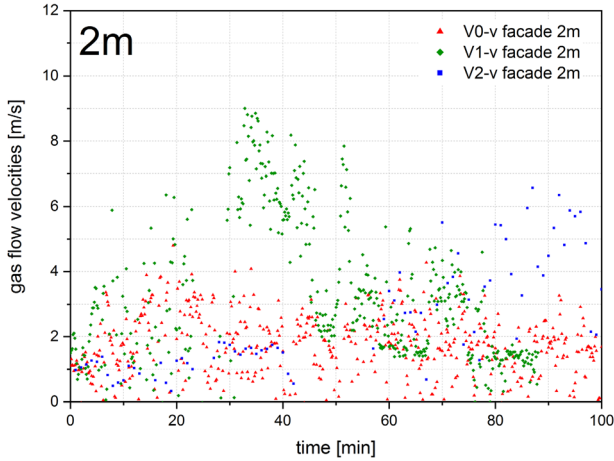


Figure 34. Comparison of the gas flow velocities on the façade at 2 m height of V0, V1 and V2.

**Table 2
Summary of the Test Results**

Test		V0	V1	V2	V3	V4
Compartment	Max. compartment gas temperature (°C)	1350	1400	1290	1250	1220
	Time to flashover (min)	9	9	8	10	10
	Duration of fully-developed fire phase (min)	31	36	34	42	45
	Onset of the beginning decay phase (min)	40	45	42	52	55
	Char fall-off on CLT walls (min)	–	85	80	–	–
	Max. HRR by movable fire load (MW)	10	8	9	16.5	16
	Start time of charring behind fire protection lining ^a (min)	–	37	63	53/75 ^b	–
	Failure time of fire protection lining ^c (min)	–	66	81	69/95 ^b	–
	Extinguishing by fire brigade (min)	–	93	92	150	65
	Self-extinguishing ^d (min)	220	–	–	–	–
Façade	Max. façade temperature (°C)	900	1080	950	1180	1160
	Max flame height (m)	5.2	5.2	5	5.7	5.5
	First flames on the façade (min)	9	9	8	10	10
	No longer flames on façade (min)	52	78	56	76	–
	Max. heat flux (kW/m ²)	55	85	61	107	109
	Max. gas flow velocity (m/s)	9.9	10.2	7.6	–	–

^aThe start time of charring behind the fire protection lining is defined as exceeding a temperature of 300°C [36]

^bFirst value for 2 × 12.5 mm, second value for 2 × 18 mm gypsum fiberboard

^cThe failure time of the fire protection lining corresponds to the time until less than 50°C difference between gas temperature in the compartment and measured temperature behind the lining is reached [37]

^dSelf-extinguishing is defined as the complete extinguishing (no smouldering) of the movable and structural fire load (construction)

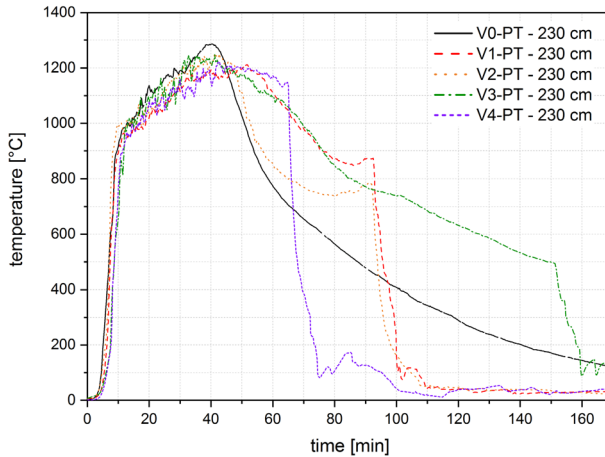


Figure 35. Comparison of the gas temperatures in the compartment at the plate thermocouple at a height of 230 cm.

Table 3 Comparison of the Fire Load Densities of the Tests Cited in Sect. 2.2

Test	Su et al. [15]	Su et al. [17]	Épernon Fire Tests [18]	Brandon et al. [24]	Kotsovinos et al. [26]	Kotsovinos et al. [29]	TIMpuls
Fire load density (MJ/m ²)	550	550	891	560	374	377	1085
Opening factor [41] (m ^{1/2})	0.03	0.03/0.06	0.050/0.032	0.062/0.25	0.071	0.039	0.094
Time to flash-over (min)	5 to 7	10 to 15	2	4 to 17	5.6 ^a	7.3 ^a	8 to 10 min

^aLocalised flashover

5. Discussion

5.1. Summary of the Test Results

The results of the tests are presented in Table 2 for further discussion.

5.2. Gas Temperature

The gas temperatures in the fire growth phase show almost no differences between non-combustible and combustible structures due to an identical movable fire load density and ignition process. This phenomenon is caused by the relatively high fire load density in the TIMpuls fire tests.

The fully-developed fire phase, which always starts at about the 10th minute of the tests, shows only minor differences in the temperature curve ($\Delta T < 150$ K) up

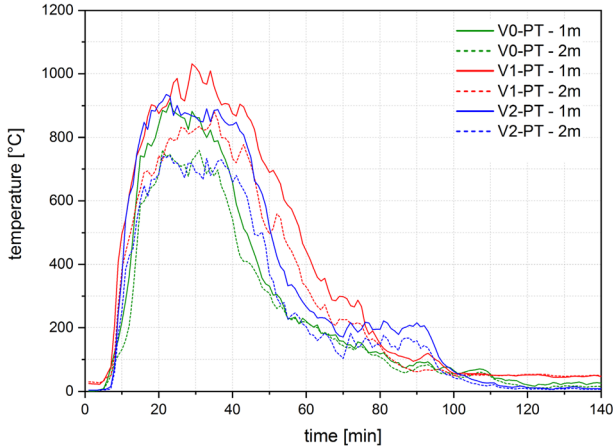


Figure 36. Comparison of the temperature-time diagrams of the plate thermocouples centered above the opening at a height of 1 and 2 m on the façade for V0, V1, V2.

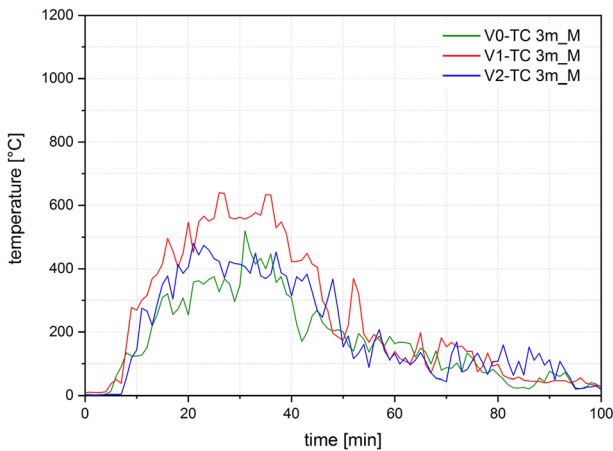


Figure 37. Comparison of the temperature-time diagrams of the thermocouples centered above the opening at a height of 3 m on the façade for V0, V1, V2.

to the 40th minute of the test. The influence of the structural fire load becomes obvious based on Fig. 35.

In the fully-developed fire phase of a ventilation-controlled fire, there is not enough oxygen available to combust all pyrolysis gases inside the fire compartment. The availability of additional fuel does not influence the conditions in the compartment, as shown in Fig. 35. As described in Sect. 2.2, other researchers have concluded that the additional fire load in the form of the structural fire load leads to an earlier flashover and an earlier fire impact on the façade. These differential observa-

tions between the TIMpuls project and other tests are due to the relatively high fire load mentioned above, see Table 3. The more movable fire load is available, the lower the influence of the structural fire load in the fire development phase.

The time of the flashover depends on many factors (geometry, opening area, arrangement of timber surfaces, etc.) and is therefore not investigated in more detail. However, it is obvious from the tests that the influence of exposed timber surfaces is lower when the fire load is increased.

5.3. Façade Temperatures

Comparing the measured temperatures on the façade, it becomes clear that the additional structural fire load leads to an increase in temperatures. It should be noted that only tests V0 to V2 can be directly compared with each other. V3 and V4 can only be evaluated with each other due to the changed geometry. When comparing V0 (reference test fully encapsulated) with V1 and V2, maximum temperature deviations averaging approx. 120°C to 200°C can be seen on the façade in the fully developed fire phase in the area of the opening, as shown in Figs. 36 and 37. This temperature increase is in a similar range to the studies of Sjöström et al. [25].

Although 100% of the wall and ceiling surfaces contributed to the fire from the middle of test V1 (37th and 66th min as shown in Table 2), an increased temperature profile is obvious beforehand. This confirms that an exposed mass timber ceiling has a greater impact on the façade than exposed mass timber walls. One possible explanation is that the flames are able to run along the combustible ceiling towards the opening in conjunction with the narrow lintel of 20 cm above the opening (floor-to-ceiling opening) in these tests.

Higher temperatures occur on the façade in test V1 than in test V2. However, it must be noted, that a sleet shower set in for a short time (approx. 10 min) during

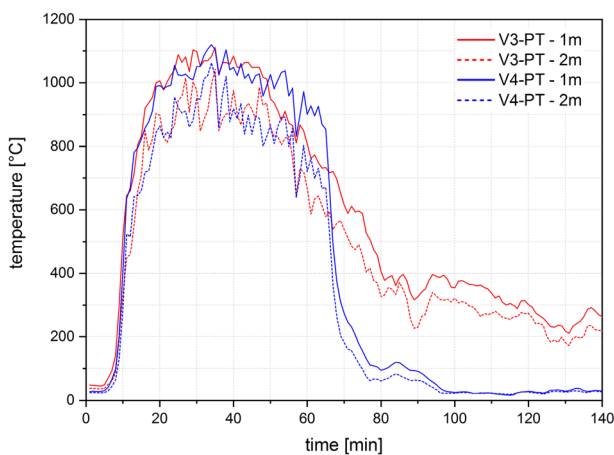


Figure 38. Comparison of the temperature-time diagrams of the plate thermocouples centered above the opening at a height of 1 m and 2 m on the façade for V3 and V4.

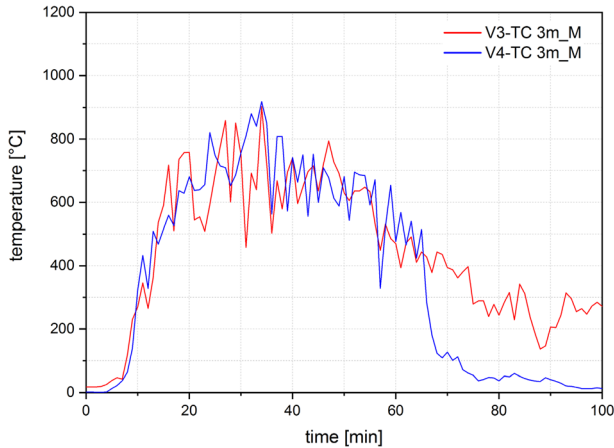


Figure 39. Comparison of the temperature-time diagrams of the thermocouples centered above the opening at a height of 3 m on the façade for V3 and V4.

the V2 test. Due to the short duration compared to the test time, the authors do not assume a critical influence for the measurement results.

Comparing V3 and V4 shows that the increase from 42% to 58% of the ratio of exposed mass timber surface does not result in any noteworthy increase in temperatures on the façade, as shown in Figs. 38 and 39.

One reason for this is that the exposed ceiling has the greatest influence on the façade and both tests had a corresponding and identical ceiling. On the other hand, the tests have a high fire load density (Table 5), which leads to a strong fire impact on the façade regardless of the exposed surfaces.

Whether an exposed ceiling has a higher impact on the façade fire exposure, especially in combination with floor-to-ceiling openings, than a percentage increase in exposed walls should be investigated further.

In order to examine the question as to whether the second storey above the fire compartment is exposed to a higher risk with regard to fire exposure along the façade in the case of exposed mass timber surfaces in more detail, the temperatures were illustrated in the center above the opening at a height of 3 m, as shown in Figs. 37 and 39. The reason for this hypothesis is that (I) the second storey above the fire compartment begins 3 m above the floor-to-ceiling opening and (II) a fast fire spread over more stories is critical for the fire brigade due to the necessary number of staff and the technical limits of e.g. dry or wet risers [42–44]. Comparing V0 and V1 shows that V1 reaches 200°C at the facade about 4 min earlier and while V0 reaches peak temperatures between 400°C and 500°C, V1 reaches temperatures above 600°C at the facade. To quantify the influence of these differences more precisely, one possible question would be which temperatures cause glass to fail. Babrauskas [45] shows that it is very difficult to predict when glass will actually break enough to fall out in a real fire. Morris [46] concludes that double-glazed windows with 6 mm thick glass fail at about 600°C.

Whether the temperature difference of approx. 200°C on average actually leads to a higher risk in reality cannot be answered conclusively. However, considering Morris' results, it seems possible.

5.4. Flame Heights

Figures 29 and 30 show that there is no significant difference in flame height between V0, V1 and V2 or between V3 and V4. Looking at the temperatures on the façade, it can be seen that although there is a difference in this series of tests in terms of the temperature of the flame, the height itself is not affected by an additional structural fire load. Differences in the comparison of V0, V1 and V2 exist at the beginning and after the 40th minute, but not in the fully developed fire. V1 and V2 have a more intense flame on the façade a few minutes before V0. The difference is greatest for V1 compared to V0. From the 40th minute, the flames on the façade of V0 decreased, and no more flames were observed on the façade from about the 53rd minute. For V2, this occurred 5 min and for V1 26 min later.

The higher deviation of V1 at the beginning, and especially from the 40 min onwards, is obviously due to the additional structural fire load (after 37 min the wall surfaces began to contribute to the fire in addition to the ceiling). Due to the additional structural fire load, the fire duration was prolonged. The wooden cribs (movable fire load) burn down more slowly due to the ventilation conditions (ventilation-controlled fire) and the additional structural fire load in the compartment. The prolonged fire causes longer-lasting flames on the façade.

These results from TIMpuls contradict the findings of Sjöström et al. [25] and Kotsovinos et al. [26]. These two studies concluded that additional structural fire load leads to an increase in flame heights. The reason for this could be the high fire load density and the large width of the opening selected in TIMpuls. Due to this high fire load density, high flames are formed independently and the influence of the additional structural fire load is thus reduced.

5.5. Heat Flux on the Façade

Figure 31 shows that V0 and V2 behave very similarly in terms of heat flux. However, there are large deviations between V0 and V1, with peak deviations of up to 35 kW/m². Because this peak deviation occurs before the 35th minute, an influence of the initially protected CLT walls can be ruled out. It can therefore be concluded that an exposed CLT ceiling leads to higher heat fluxes on the façade than an exposed mass timber wall. This theory is also supported by Bartlett et al. [9]. As in [9], it is assumed that more unburnt gases leave the compartment directly without mixing with the gases in the compartment with an exposed ceiling, and consequently burn in the plume.

The results from the Épernon Fire Tests [18], that the incident heat flux on the façade is approximately 3 times greater when a timber ceiling is used instead of a concrete ceiling, could not be confirmed. The reason for this could again be the different fire load densities and the width of the opening. The influence of the exposed ceiling decreases with a high fire load density and a large width of the opening (opening factor in Table 3), as in the TIMpuls tests.

Figure 32 shows that an increase of the exposed timber surface does not lead to any differences in the course at the beginning and during the fully developed fire phase.

5.6. Gas Flow Velocities

Figures 33 and 34 compare the gas flow velocities on the façade at a height of 1 and 2 m for V0, V1 and V2.

It can be seen that V0, V1 and V2 have similar gas flow velocities at 1 m height. This is because the persistent flame is always located in this area.

Comparing the gas velocities at a height of 2 m shows that V0 and V2 have similar results. V1 has higher results in a direct comparison. The fact that the wall lining starts to fail at the 37th minute and both wall and ceiling surfaces contributed to the fire could explain the increase in gas velocity.

6. Conclusion and Outlook

The aim of this study was to investigate whether exposed timber surfaces or initially protected timber components can lead to more critical effects on the façade.

Five full-scale fire tests were carried out to investigate this. Three tests in a square compartment (4.5×4.5 m) and two in a double-width compartment (4.5×9 m). The tests were conducted with a high, movable fire load density (1085 MJ/m^2). While the first test was carried out in a fully encapsulated (non-combustible) compartment, the exposed timber surfaces were subsequently increased. The influence of exposed or only initially protected timber surfaces on the fire impact on the façade was investigated using the measured gas temperature, HRR, temperature on the façade, flame heights along the façade, heat flux and velocities along the façade.

There are almost no differences in the gas temperatures in the growth phase of the fire, and there are only minor differences in the temperature curves in the fully-developed fire phase. The influence of the structural fire load becomes visible afterwards. The course of the gas temperature in the decay phase is thus primarily defined by the exposed, or only initially protected timber surfaces involved in the fire (structural fire load).

In the fully-developed fire phase of a ventilation-controlled fire, the lack of oxygen governs the combustion. The more movable fire load is available, the lower the influence of the structural fire load in the fire development phase.

Additional structural fire load leads to an increase in temperatures on the façade. In these tests, maximum temperature deviations increases averaging approx. 120°C to 200°C occurred on the façade in the fully-developed fire phase. An exposed mass timber ceiling has a greater impact on the façade than exposed mass timber walls. The specific influence an exposed ceiling has on the façade fire exposure requires further investigation.

There is no significant difference in flame height between the tests. Due to the additional structural fire load, the fire is lengthened in time. The prolonged fire causes longer-lasting higher flames on the façade.

An exposed mass timber ceiling leads to higher heat fluxes on the façade than an exposed mass timber wall. The theory that the incident heat flux on the façade is approximately three times greater when a mass timber ceiling is used instead of a non-combustible ceiling could not be confirmed. The reason for this could again be the different fire load densities and the width of the opening.

Furthermore, the results of the gas flow velocity measurement on the façade support the hypothesis that the gas velocities increase with a growing structural fire load.

Overall, it is evident that the internationally available findings from full-scale fire tests are currently insufficient to conclusively clarify this issue. Since many factors such as geometry, opening factor [29, 47], arrangement of timber surfaces [47], fire load density, compartment size, protection times of linings, etc. play a decisive role, it is not possible to make any general statements at the present time. In order to further investigate and quantify this important topic, additional full-scale tests are necessary. The series of tests [48] or the unpublished parts of the CodeRed test series [26, 29] could provide further results. Unfortunately, the measurement results on the façades have not yet been published.

Acknowledgements

The research has been funded by the German Federal Ministry of Food and Agriculture through the project management agency Fachagentur Nachwachsende Rohstoffe e.V. (FNR). The Bavarian Carpenters' Guild Association (Landesinnungsverband des Bayerischen Zimmererhandwerks) coordinated co-financing by the timber industry. All research partners staff from Technische Universität Braunschweig, Magdeburg-Stendal University of Applied Sciences and the Institute of Fire and Civil Protection Heyrothsberge involved in these tests are acknowledged. The following research staff that helped to carry out these tests successfully are gratefully acknowledged: Sven Brunkhorst, Daniel Butscher, Franziska Heumann, Björn Kampmeier, Christoph Kurzer, Markus Lechner, Michael Neske, Felix Steeger, Stefan Winter and Jochen Zehfuß as well as the students. We would also like to extend our heartfelt thanks to the TUM Fire Brigade Garching and Gump & Maier GmbH for their technical support.

Funding

Open Access funding enabled and organized by Projekt DEAL.

Declarations

Conflict of interest All authors declare that they have no conflict of interest.

Open Access

This article is licensed under a Creative Commons Attribution 4.0 International License, which permits use, sharing, adaptation, distribution and reproduction in any medium or format, as long as you give appropriate credit to the original author(s) and the source, provide a link to the Creative Commons licence, and indicate if changes were made. The images or other third party material in this article are included in the article’s Creative Commons licence, unless indicated otherwise in a credit line to the material. If material is not included in the article’s Creative Commons licence and your intended use is not permitted by statutory regulation or exceeds the permitted use, you will need to obtain permission directly from the copyright holder. To view a copy of this licence, visit <http://creativecommons.org/licenses/by/4.0/>.

Appendix

An overview of the individual wall and ceiling structures used in the TIMpuls compartment full-scale fire tests is shown in Table 4.

Table 4
Overview of the Timber Constructions

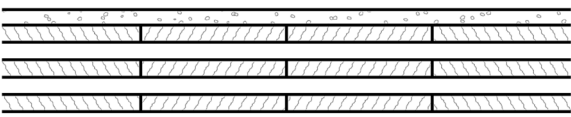
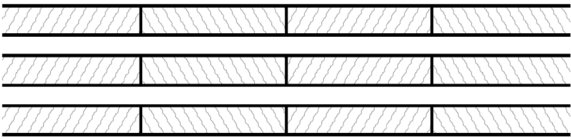
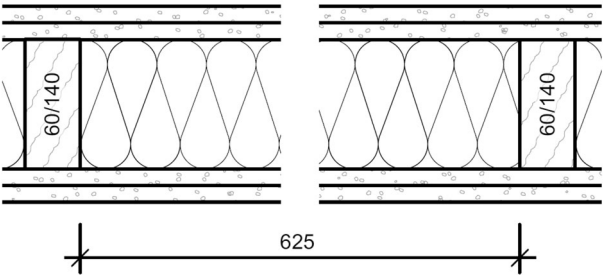
Wall structures	
	<p>100 mm cross-laminated timber wall (five layers 20 20 20 20 20 mm) with 18 mm gypsum plasterboard type F/gypsum fiberboard</p>
	<p>150 mm cross-laminated timber wall (five layers 34 24 34 24 34 mm)</p>
	<p>140 mm light timber frame with 2 × 18 mm gypsum plasterboard type F/gypsum fiberboard</p>

Table 4
continued

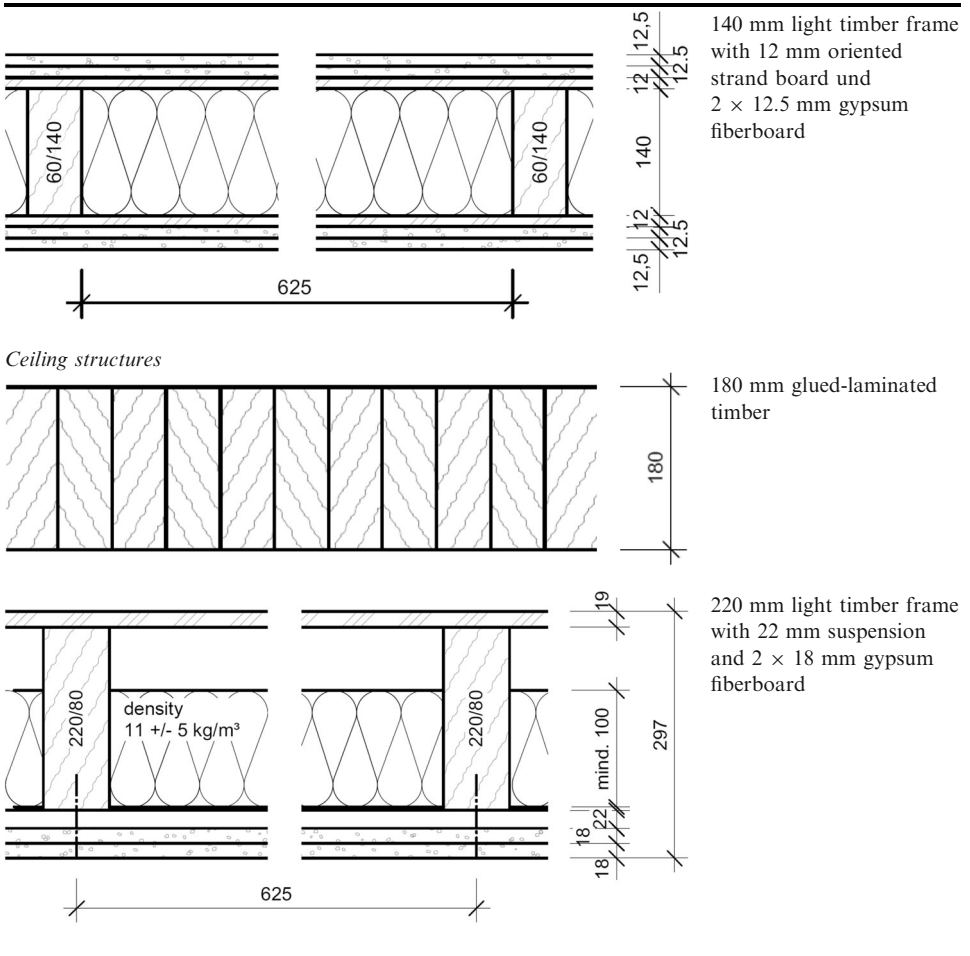


Table 5 shows the fire load density to be used according to Eurocode 1 or the National Annex.

Table 6 shows the mean values of the weather data over the test time measured per minute.

Table 7 shows the parameters for determining the HRR via the charring rate.

Table 5
Comparison of Statistical Fire Load Densities for Dwellings in Europe

EN 1991-1-2 [41]	Germany [31]	Denmark [49]	France [50]	Great Britain [51, 52]	Ireland [53]	Italy [54]
948 MJ/m ²	1085 MJ/m ²	200 MJ/m ^{2a}	930 MJ/m ²	870 MJ/m ²	870 MJ/m ²	948 MJ/m ²
80% fragile	90% quantile	80% fragile	90% quantile	80% fragile	80% fragile	80% fragile

^aRelated to A_t, total area of enclosure (walls, ceiling and floor, including openings)

Table 6
Weather Data from the Weather Station Located Directly Next to the Test Area, Shown As Mean Values of the Minute Measurements over the Test Period for Different Heights

Height	Temperature (°C)	Wind speed (km/h)						Air pressure (hPa)
	1 m	0.2 m	0.5 m	1 m	2 m	5 m	10 m	–
V0	– 1.0	1.0	1.0	1.0	1.2	1.3	1.5	962
V1	6.8	0.7	0.7	1.1	1.2	1.4	1.3	954
V2	3.4	0.9	0.8	1.3	1.4	1.6	1.8	951
V3	10.1	1.4	1.7	1.8	1.8	1.9	2.0	961
V4	– 5.0	2.6	2.5	2.9	2.9	3.0	3.1	971

Table 7
Parameters for Determining the Heat Release Rate via the Charring Rate

Components	300°C on the timber surface	≤ 50°C deviation behind the lining to the compartment	Residual cross-section	Timber surface area
V1				
Exposed GLT ceiling	6 min	–	107 mm	20.3 m ²
Initially protected CLT walls	37 min	66 min	70 mm	37.9 m ²
V2				
Exposed CLT walls	6 min	–	79 mm	10.8 m ²
LTF walls	63 min	81 min	115 mm	1.6 m ²
LTF ceiling	63 min	81 min	205 mm	2.9 m ²
V3				
Exposed GLT ceiling	7 min	–	107 mm ^a	40.5 m ²
LTF wall	53 min	69 min	115 mm ^a	10.8 m ²
(2 × 12.5 mm GF + 12 mm OSB)				OSB + 1.0 m ²
LTF wall (2 × 18 mm GPF/GF + 12 mm OSB)	75 min	95 min	8 mm OSB ^a	10.8 m ²
LTF wall (2 × 18 mm GPF/GF)	75 min	95 min	128 mm ^a	2.2 m ²
V4				
Exposed GLT ceiling	7 min	–	125 mm	40.5 m ²
Exposed GLT column	7 min	–	175 × 175 mm	2.5 m ²
Exposed GLT beam	7 min	–	265 × 185 mm	6.1 m ²
Exposed CLT wall	7 min	–	100 mm	10.8 m ²
LTF wall (2 × 18 mm GPF/GF)	–	–	–	–

^aDetermined up to the 90th minute via the 300°C isotherm of the thermocouples in the component

Figures 40, 41, 42, and 43 shows the results of the two methods for determining the HRR (mass loss vs. charring rate) for each test.

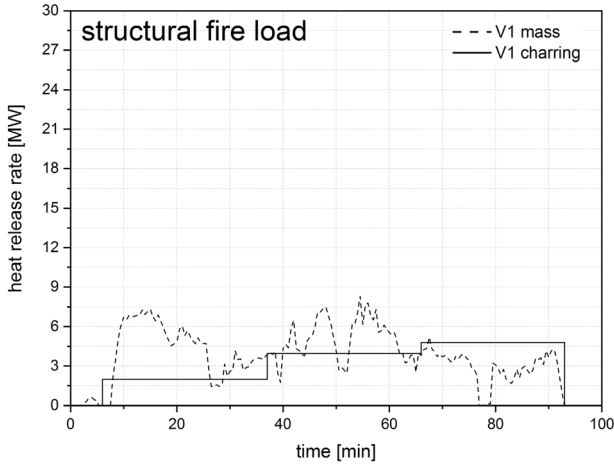


Figure 40. Results of the two methods for determining the heat release rate (mass loss vs. charring rate) for V1.

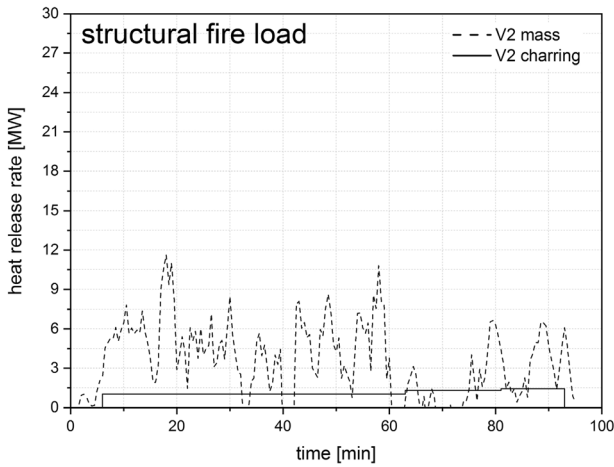


Figure 41. Results of the two methods for determining the heat release rate (mass loss vs. charring rate) for V2.

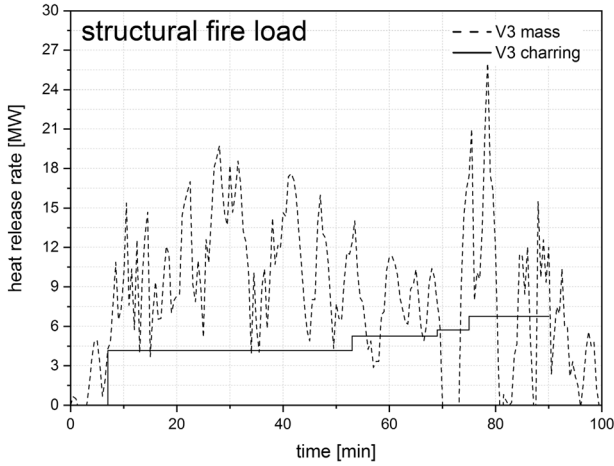


Figure 42. Results of the two methods for determining the heat release rate (mass loss vs. charring rate) for V3.

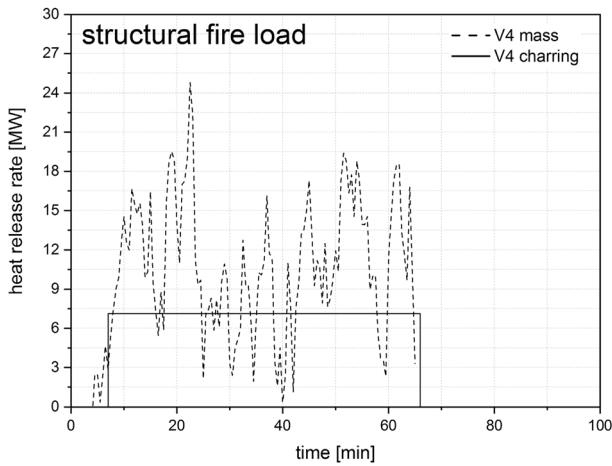


Figure 43. Results of the two methods for determining the heat release rate (mass loss vs. charring rate) for V4.

SUPPLEMENTARY INFORMATION

The online version contains supplementary material available at <https://doi.org/10.1007/s10694-022-01346-8>.

References

1. Reitan NK, Friquin KL, Mikalsen RF (2019) Brannsikkerhet ved bruk av krysslaminert massivtre i bygninger—en litteraturstudie. Rep. 2019:09 RISE Research Institutes of Sweden, Trondheim
2. Friquin KL, Reitan NK, Mikalsen RF (2019) Fire exposure on façades of cross-laminated timber buildings—a review. In: FSF 2019—3rd international symposium on fire safety of façades, Paris
3. Brandon D, Just A, Andersson P, Östman B (2018) Mitigation of fire damages in multi-storey timber buildings - statistical analysis and guidelines for design. Rep. RISE Report 2018:43, RISE Research Institutes of Sweden, Stockholm
4. Göldner M (2021) Evaluation of fire and hazard prevention measures - Part 4: Determination and evaluation of quantified propagation factors (Evaluierung der Maßnahmen des vorbeugenden Brand- und Gefahrenschutzes—Teil 4: Ermittlung und Bewertung quantifizierter Ausbreitungsfaktoren). Master Thesis, Technical University of Munich
5. Maiworm B (2021) Göldner M (2021) Einsatzstellenbegehungen—Fokus: Hat das Gebäude funktioniert?. Braunschweiger Brandschutz-Tage 241:63–82
6. Gorska C (2019) Fire dynamics in multi-scale timber compartments. Dissertation, The University of Queensland
7. Gorska C, Hidalgo JP, Torero JL (2021) Fire dynamics in mass timber compartments. *Fire Saf J*. <https://doi.org/10.1016/j.firesaf.2020.103098>
8. Nothard S, Lange D, Hidalgo J P, Gupta V, McLaggan M S (2020) The response of exposed timber in open plan compartment fires and its impact on the fire dynamics. In: SiF 2020—The 11th international conference on structures in fire, Brisbane. <https://doi.org/10.14264/5d97785>
9. Bartlett AI, Kanellopoulos G, Law A (2019) Heat flux distribution on a facade from timber-lined compartments. In: 15th International conference and exhibition on fire science and engineering (Interflam 2019), 1995–2002, London
10. Berger H (2021) Investigation of the effects between full scale and small scale fire tests (Untersuchung der Skalierungseffekte bei Brandversuchen). Master Thesis, Technical University of Munich
11. Maag T, Fontana M (2000) Brandversuche an Modulhotels in Holzbauweise. Report, Swiss Federal Institute of Technology ETH Zurich, Zurich. <https://doi.org/10.3929/ethz-a-004031004>
12. Frangi A, Fontana M (2005) Fire performance of timber structures under natural fire conditions. *Proc Fire Saf Sci* 8:279–290. <https://doi.org/10.3801/IAFSS.FSS.8-279>
13. Su J, Loughheed GD (2014). Fire safety summary - Fire research conducted for the project on mid-rise wood construction. Client Report A1-004377.1, National Research Council Canada
14. Hakkarainen T (2002) Post-flashover fires in light and heavy timber construction compartments. *J Fire Sci* 20:133–175. <https://doi.org/10.1177/0734904102020002074>
15. Su J, Leroux P, Lafrance P-S, Berzins R, Gratton K, Gibbs E, Weinfurter M (2018). Fire testing of rooms with exposed wood surfaces in encapsulated mass timber construction. Client Report A1-012710.1, National Research Council Canada

16. Hadden RM, Bartlett AI, Hidalgo JP, Santamaria S, Wiesner F, Bisby LA, Deeny S, Lane B (2017) Effects of exposed cross laminated timber on compartment fire dynamics. *Fire Saf J* 91:480–489. <https://doi.org/10.1016/j.firesaf.2017.03.074>
17. Su J, Lafrance P-S (2018). Fire safety challenges of tall wood buildings—phase 2: task 2 & 3—cross laminated timber compartment fire tests. NFPA Rep. No. FPRF-2018-01. NRC Rep. No. A1-012710.1, National Research Council Canada
18. Épernon Fire Tests Programme (2020) Synthesis Report; Report No. EFTP-2020/01, October 13, 2020. <http://www.epernon-fire-tests.eu/>
19. Bartlett A, Law A, McNamee RJ, Zehfuss J, Mohaine S, Tessier C, Bisby L (2019) Heat fluxes to a façade resulting from compartment fires with combustible and non-combustible ceilings. In: FSF 2019—3rd international symposium on fire safety of façades, Paris
20. Robert F et al (2019) ÉPERNON FIRE TESTS PROGRAMME—Test Report No. 013598: CLT slab (Natural Fire Test—Scenario 2), CERiB FireTesting Centre, France. <http://www.epernon-fire-tests.eu>
21. Robert F et al (2019) ÉPERNON FIRE TESTS PROGRAMME—Test report No. 013597: CLT slab (Natural Fire Test—Scenario 2), CERiB FireTesting Centre, France. <http://www.epernon-fire-tests.eu>
22. Robert F et al (2019) ÉPERNON FIRE TESTS PROGRAMME—Test Report No. 013599: CLT slab (Natural Fire Test—Scenario 2), CERiB FireTesting Centre, France. <http://www.epernon-fire-tests.eu>
23. Robert F et al (2019) ÉPERNON FIRE TESTS PROGRAMME - Test report n° 013600: CLT slab (Natural Fire Test—Scenario 2), CERiB FireTesting Centre, France. <http://www.epernon-fire-tests.eu>
24. Brandon D, Sjöström J, Temple A, Hallberg E, Kahl F (2021) Final project report—fire safe implementation of visible mass timber in tall buildings—compartment fire testing. RISE Report 2021:40, RISE Research Institutes of Sweden
25. Sjöström J, Brandon D, Temple A, Hallberg E, Kahl F (2021) Exposure from mass timber compartment fires to façades. RISE Report 2021:39, RISE Research Institutes of Sweden
26. Kotsovinos P, Rackauskaite E, Christensen E, Glew A, O’Loughlin E, Mitchell H, Amin R, Robert F, Heidari M, Barber D, Rein G, Schulz J (2022) Fire dynamics inside a large and open-plan compartment with exposed timber ceiling and columns: CodeRed #01. *Fire Mater.* <https://doi.org/10.1002/fam.3049>
27. Rackauskaite E, Bonner M, Restuccia F et al (2021) Fire experiment inside a very large and open-plan compartment: x-ONE. *Fire Technol* 58:905–939. <https://doi.org/10.1007/s10694-021-01162-6>
28. Heidari M (2021) Travelling fires methodology and probabilistic design of structures. PhD thesis. Imperial College London
29. Kotsovinos P, Christensen EG, Rackauskaite E, Glew A, O’Loughlin E, Mitchell H, Amin R, Robert F, Heidari M, Barber D, Rein G, Schulz J (2022) Impact of ventilation on the fire dynamics of an open-plan compartment with exposed timber ceiling and columns: CodeRed #02. *Fire Mater.* <https://doi.org/10.1002/fam.3082>
30. Engel T, Brunkhorst S, Steeger F, Butscher D, Kurzer C, Werther N, Winter S, Zehfuß J, Kampmeier B, Neske M (2022) Schlussbericht zum Verbundvorhaben TIMpuls—Brandschutztechnische Grundlagenuntersuchung zur Fortschreibung bauaufsichtlicher Regelungen im Hinblick auf eine erweiterte Anwendung des Holzbaus. Fachagentur Nachwachsende Rohstoffe; Gülzow-Prüzen. <https://doi.org/10.14459/2022md1661419>

31. German Institute for Standardization (2015) DIN EN 1991-1-2/NA National Annex—Nationally determined parameters—Eurocode 1: actions on structures—Part 1–2: general actions—actions on structures exposed to fire. German Institute for Standardization, Berlin
32. European Committee for Standardization (2013) EN 60584-1 Thermocouples—Part 1: EMF specifications and tolerances (IEC 60584-1:2013). European Committee for Standardization, Brussels
33. European Committee for Standardization (2020) EN 1363-1:2020 Fire resistance test—Part 1: general requirements. European Committee for Standardization, Brussels
34. Starke H (2009) Kalibrierung von bidirektionalen Sonden—calibration of bidirectional probes. Jahresbericht 2006/2007/2008, IdF Sachsen-Anhalt, Heyrothsberge 2009
35. Brunkhorst S, Zehfuß J, Engel T, Kurzer C, Werther N, Steeger F, Butscher D (2021) TIMpuls Grossversuche an Holzbauten. Braunschweiger Brandschutz-Tage 2021
36. Standard E (2009) Eurocode 5: Design of timber structures—part 1–2: general—structural fire design; German version EN 1995-1-2:2004 + AC:2009. European Committee for Standardization, Brussels
37. European Committee for Standardization (2019) EN 13381-7 Test methods for determining the contribution to the fire resistance of structural members—Part 7: applied protection to timber members. European Committee for Standardization, Brussels
38. Ahrens J (2021) Influence of the immobile fire load on the fire effect on the façade (Einfluss der immobilen Brandlast auf die Brandeinwirkung auf der Fassade). Master Thesis, Technical University of Munich
39. Häggkvist A, Sjöström J, Wickström U (2021) Using plate thermometer measurements to calculate incident heat radiation. *J Fire Sci* 31(2):166–177. <https://doi.org/10.1177/0734904112459264>
40. Ingason H, Wickström U (2007) Measuring incident radiant heat flux using the plate thermometer. *Fire Saf J* 42:161–166. <https://doi.org/10.1016/j.firesaf.2006.08.008>
41. European Standard (2009) Eurocode 1: Actions on structures—Part 1–2: general actions—actions on structures exposed to fire; EN 1991-1-2:2002 + AC:2009
42. Engel T, Werther N (2020) Analyse der zulässigen Brandausbreitung über die Fassade. *Bautechnik* 97:558–565. <https://doi.org/10.1002/bate.202000007>
43. European Commission (1994) Communication of the Commission with regard to the interpretative documents of Council Directive 89/106/EEC (94/C 62/01). Official Journal of the European Communities
44. NFPA (2016) NFPA 14—Standard for the Installation of Standpipe and Hose Systems
45. Babrauskas V (2010) Glass breakage in fires. https://fireevacuationplan.ru/articles/data/Folder/to139_GlassBreak.pdf. Accessed 16 May 2022
46. Morris B (1999) Fire spread in multi-storey buildings with glazed curtain wall facades. (LPR 11: 1999), Loss Prevention Council, Borehamwood, England
47. Brunkhorst S, Zehfuß J (2020) Experimental and numerical analysis of fire development in compartment fires with immobile fire load. In: International scientific conference on woods & fire safety. https://doi.org/10.1007/978-3-030-41235-7_28
48. Hopkin D, Wegrznski W, Spearpoint M, Fu I, Krenn H, Sleik T, Gorska C, Stapf G (2022) Large-scale enclosure fire experiments adopting CLT slabs with different types of polyurethane adhesives: genesis and preliminary findings. *Fire* 5:39. <https://doi.org/10.3390/fire5020039>
49. DS/EN 1991-1-2 DK NA:2014 National Annex to Eurocode 1: actions on structures—Part 1–2: general actions—actions on structures exposed to fire
50. NF EN 1991-1-2/NA:2007 Annexe nationale à la Eurocode 1—Actions sur les structures—Partie 1–2 : Actions générales—Actions sur les structures exposées au feu

51. NA to BS EN 1991-1-2:2002 UK National Annex to Eurocode 1: Actions on structures—Part 1–2: general actions—actions on structures exposed to fire
52. PD 6688-1-2:2007 Background paper to the UK National Annex to BS EN 1991-1-2
53. N.A. to I.S. EN 1991-1-2:2002 Irish National Annex to Eurocode 1: actions on structures—Part 1–2: general actions—actions on structures exposed to fire
54. Appendice Nazionale Italiana alla UNI EN 1991-1-2:2005 Parametri adottati a livello nazionale da utilizzare per le strutture esposte al fuoco

Publisher's Note Springer Nature remains neutral with regard to jurisdictional claims in published maps and institutional affiliations.